

High Power Impulse Magnetron Sputtering for Industrial Applications: Deposition of Chromium Films on Inclined Surfaces

*G. Greczynski and J. Böhlmark, Chemfilt Ion Sputtering AB, Linköping, Sweden;
Y.T. Pei, C.Q. Chen and J.T.M. De Hosson, Department of Applied Physics, Netherlands Institute for Metals Research, University of Groningen, Groningen, The Netherlands; and
M. Alunovic and R. Cremer, CemeCon AG, Würselen, Germany*

ABSTRACT

High Power Pulsed Magnetron Sputtering (HIPIMS or HPPMS) is a magnetron sputtering technique that draws increasing interest due to the ability to form droplet-free films out of highly ionized vapor of the target material. Invented by Kouznetsov in 1999 (US patent US6296742), HIPIMS has gone the long way and is nowadays entering the stage of commercial applications. In this work chromium films were deposited by HIPIMS, as well as, by conventional DC magnetron sputtering on a set of substrates with an inclination angle of 0°, 90° and 180° degrees with respect to the target surface normal. The background gas pressure and the average power to the cathode were varied during depositions. Cross-sectional scanning electron microscopy was used for microstructure characterization of produced films and for the determination of deposition rates. The chromium ion content in the plasma, monitored with optical emission spectroscopy, increases with increasing target peak power. Results reveal also quite dramatic quality difference between films grown on tilted substrates by HIPIMS and by conventional DC sputtering.

INTRODUCTION

High power impulse magnetron sputtering (HIPIMS) is a sputtering technique that has drawn much attention from both industry and academia in the recent years [1]. The method has been previously reported by Kouznetsov *et al* [2]. HIPIMS is an alternative technique for ion assisted thin film growth and surface engineering. It relies on the creation of a high-density plasma in front of the sputtering source, ionizing a large fraction of the sputtered atoms. The increase in plasma density is achieved by increasing the peak power applied to the target in short (typically less than 100 μ s) pulses, with a low duty factor (a few percent). Since the thermal load of the target is limited by the average power rather than the peak power, the peak power during the active discharge can be very high. The applied voltage can reach a peak value of a couple of kV, resulting in peak discharge current density on the order of a few A/cm² and a peak power density of several kW/cm². These high peak power levels result in electron densities exceeding 10¹⁹ m⁻³ surrounding the magnetron [3-5]. The high density of electrons increases the probability for electron impact ionization of the sputtered atoms, and results in a highly ionized flux of target material [2,4,6]. Ionization levels ranging from 4.5% for carbon [7] up to over 90% for titanium [6] has been

reported. This wide spread is primarily due to the factors that govern the probability of sputter atom being ionized, namely first ionization potential of the sputtered species and the cross section for the electron-impact ionization. In addition the details of the measurement setup (location of the probe, etc.) and used technique play a role.

The high degree of ionization opens new opportunities, since the ions may be controlled by the use of electric and magnetic fields [8]. Also, the energy of the ions arriving at a surface may be controlled by the use of a substrate bias, which strongly affects the properties of the growing film [9]. The latter effect is particularly efficient if the bombarding ions are at the same time the constituents of the growing film (as opposite to working gas ions) due to more efficient momentum transfer. The high degree of ion content together with the fact that the vast majority of ions is created in the vicinity of the target surface (in contrast to conventional I-PVD where the secondary plasma is created away from the target to ionize the flux of sputtered atoms on its way to the substrate [10]) is a reason for the main drawback of this technique - the commonly observed drop in the deposition rate [11]. The effect is believed to be caused by the fact that a certain fraction of the ionized target material is attracted back to the target, which results in severe rate drop especially for materials characterized by low self-sputtering yields [12,13].

In this paper we put the rate drop issue at a different perspective by investigating the films grown on substrates not necessarily facing the target. The results are presented for chromium films deposited by HIPIMS, as well as, by conventional DC magnetron sputtering, on a set of substrates with an inclination angle of 0°, 90° and 180° degrees with respect to the target surface normal. Data were obtained at different peak power levels and for various pressures of the working gas. The ion content in the plasma was monitored by optical emission spectroscopy (OES).

EXPERIMENTAL

All the depositions were performed in the state of the art CC800/9 coating system manufactured by CemeCon AG in Germany. The relevant details of the system configuration can be found on the manufacturer web site [14]. Due to the nature of the experiment only one out of four cathodes

mounted in the system was used. A rectangular chromium target of dimensions 88×500 mm² was used. The chamber was evacuated to the base pressure of 10⁻⁵ Torr. Argon of purity 99.9997% was introduced through a leak valve to start and maintain the discharge. The cathode was operated by a HIPIMS power supply Sinex 3 manufactured by Chemfilt Ion sputtering AB, Sweden, capable of delivering 2 kV peak voltage pulses and the average power of up to 10 kW. In the case of industrial size targets like used in this experiment the exact shape of current and voltage waveforms is to a great extent determined by the size of the capacitor bank used in the powering unit. As can be seen in Figure 1, the voltage is not constant throughout the pulse in the present set up, but rather drops from the peak value reached right at the beginning of the pulse (before any current flows) as the charge is withdrawn from the capacitor bank after the ignition of the discharge. The resulting target current is thus proportional to the rate at which voltage drops at the target according to $I = C \times dU/dt$, where C stands for capacitance, I and U are target current and target voltage. As soon as the target voltage becomes too low to sustain discharge, current goes down to zero limiting the power pulse down to about 80 μs. In this way the target area sets the limit for duration of the current (and power) pulses. It can also be seen from the data in Figure 1 that as soon as the peak target voltage increases above 850-900V the current peaks consists of two components. This double current peak has also been observed previously on laboratory scale systems for chromium [15] and tantalum [16], but its origin is not fully understood.

For this work the pulse frequency was set to 300 Hz for all the depositions, resulting in the duty cycle of ca. 2% and the average power between 1.6 kW and 5.5 kW. The peak power levels achieved in this experiment were between 140 kW and 750 kW. Hence the highest peak power density was 1.7 kW/cm² (calculated for the whole target area) while the average power density did not exceed 12.5 W/cm².

The target current was measured with a Tektronix CT-04 high current transformer together with a Tektronix TCP202 current probe mounted right at the connection to the vacuum chamber. A Tektronix P6015 high voltage probe was used to measure the cathode voltage. Current and voltage waveforms were recorded with the Picoscope 3000 real time digital storage PC oscilloscope from Pico Technology.

The chromium films were deposited on silicon wafers that were cleaned in acetone and isopropanol using ultrasonic bath. For each deposition three substrates were mounted on the sample holder that was located 7 cm away from the target surface and symmetrically with respect to the race tracks of the rectangular target. The substrates were mounted with a vertical spacing of ca. 1 cm and tilted by 0° (facing

the target), 90° (along the normal to the target surface) and 180° degrees (facing away from the target). Samples were on the floating potential during depositions and no external heating was used.

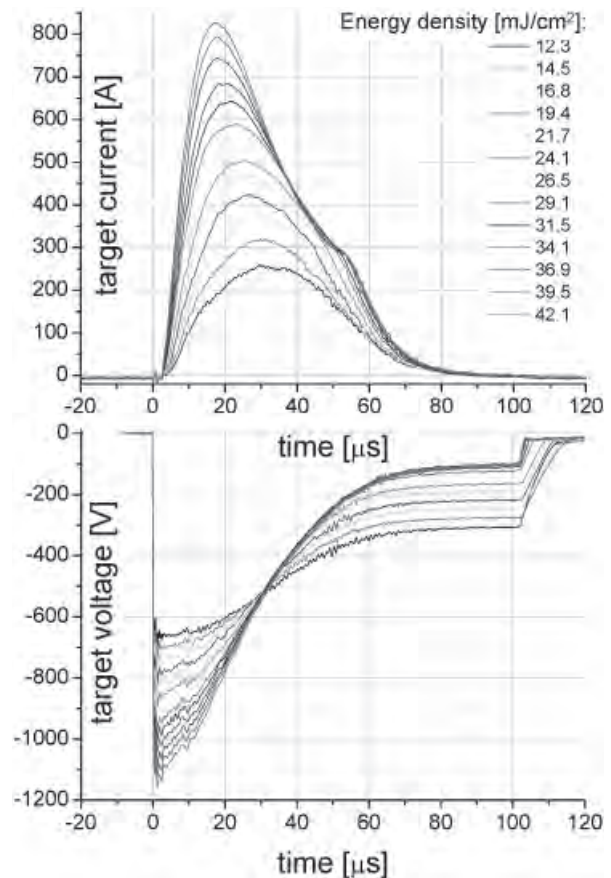


Figure 1: Target current (top) and target voltage (bottom) waveforms recorded at 3 mTorr argon gas pressure. The parameter that is varied here is the output voltage of the power supply, what has an effect on the peak value of the target voltage and, in consequence, on the peak target current. The energy density (per pulse) indicated in the legend box is basically the product of current and voltage traces integrated over the time period of one pulse (100 μs) and divided by the whole area of the target.

The optical emission from the plasma was measured in the line-of-sight geometry through a port window of the chamber and the probe was directed towards the race track. A spectrometer (Mechelle Sensicam 900) connected to a collimator via an optical fiber was used to record the emission from the plasma. The spectral range of the spectrometer was 300-1100 nm. The OES data were acquired at argon gas pressures ranging between 0.5 and 10 mTorr and for different target voltages (implying different peak power levels). The shutter speed of the spectrometer was set to 100ms, meaning that all data were time-averaged over ca. 30 pulses.

RESULTS AND DISCUSSION

Some examples of OES data are shown in Figure 2. All the spectra were recorded at 3 mTorr argon gas pressure and the peak target voltage was varied between 600V and 1200V. This variation in target voltage corresponds to significant changes in discharge current (see Figure 1) or, in other terms, energy released in each pulse. If the whole target area is taken into account, the energy density per pulse increases from 12.3 mJ/pulse up to 42.1 mJ/pulse as the target peak voltage increases from 600V up to 1200V. It can be seen in the left panel of this figure that the emission from singly ionized Cr is detected at all power levels. All lines are coupled to $4s \rightarrow 4p$ transitions with the excitation energies lying between 6.05eV and 6.16 eV. The right panel of the same figure shows the emission from Cr neutrals with similar excitation energies (5.65 eV). Emission from both ions and neutrals increases as more energy is delivered to the system in each pulse predominantly due to increased number of emitting species residing in the plasma (more metal gets sputtered with increasing target voltage), as well as, increased number of free electrons. However, the emission intensity from Cr^+ ions increases roughly by a factor of eight, whereas the signal from Cr neutrals increases only about three times as the peak voltage on the cathode doubles (from 600 V to 1200 V). Since the excitation energy in both cases is close to each other, one can conclude qualitatively that the relative amount of Cr^+ ions with respect to Cr atoms increases significantly with increasing energy per pulse. This point is illustrated further in Figure 3 where the emission intensities of the strongest lines corrected for transition probabilities are plotted for Cr^+ ions and Cr neutrals, respectively, versus energy per pulse for various argon gas pressures. The emission lines chosen for comparison are CrI at 399.1 nm and CrII at 336.8 nm. It is clearly observed that there is a linear relation between the intensity of optical emission of both Cr^+ ions and Cr neutrals and the energy per pulse. Especially, the slope of the linear function for Cr^+ ions is much larger than that of Cr neutrals, indicating a faster increase of Cr^+ ions flux with increasing the energy per pulse. Moreover the ion-to-neutral emission ratio seems to be independent of the working gas pressure. For the sake of completeness corresponding measurements were also carried for DC magnetron sputtering chromium (not shown here). However, no emission from Cr ions was detected in this case.

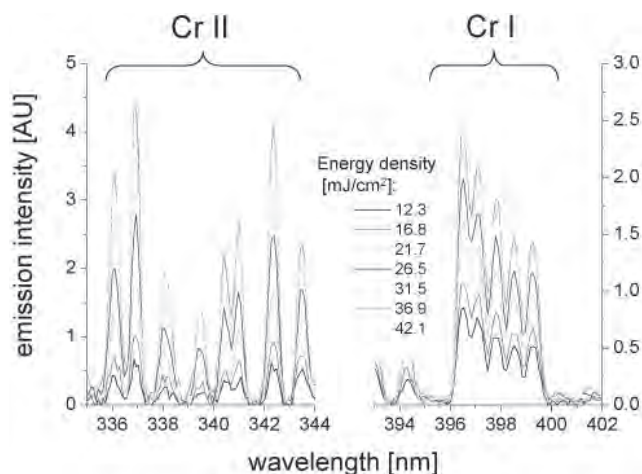


Figure 2: The optical emission spectra recorded for increasing energy density per pulse. A series of lines in the left panel originates from singly charged chromium ions whereas all lines in the right panel are due to chromium neutrals.

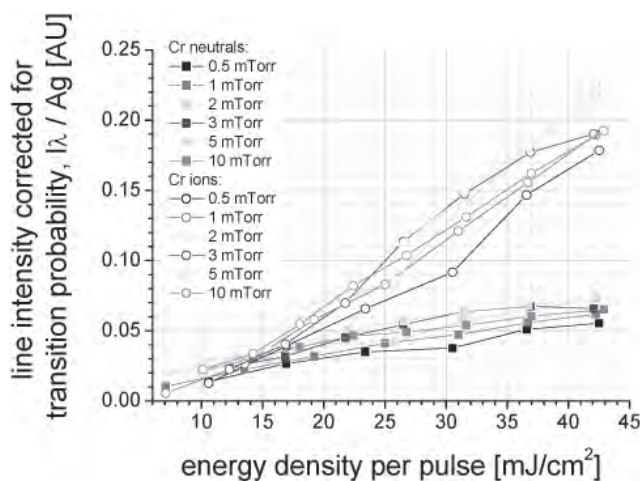


Figure 3: The dependence of emission intensity from CrI (399.1 nm) and Cr II (336.8 nm) lines on the energy density per pulse. The working gas pressure was varied between 0.5 mTorr and 10 mTorr. In order to facilitate comparison line intensities are corrected for transition probability of the spontaneous emission (A) and the upper level degeneracy (g).

The detailed quantification of the OES data is rather complicated due to a number of reasons, including the dynamic nature of the discharge, lack of thermodynamic equilibrium (undefined electron temperature), experimental setup (line-of-sight geometry), etc. It should also be emphasized that the time-averaged spectra do not reflect the fact that the degree of ionization of the sputtered metal atoms may vary during the pulse giving rise to variations in the ion-to-neutral emission ratio, as was observed in other laboratories [4].

Figure 4 summarizes the deposition rates (derived from SEM cross-sections) under various sputtering conditions for substrates oriented at the inclination angle of 0° (facing the target), 90° (along the normal to the target surface) and 180° degrees (facing away from the target). In order to facilitate the comparison data was, in each case, normalized to the deposition rate obtained on the substrate facing the target. All depositions were done at the same average power of 3.3 kW. When comparing HIPIMS to DC sputtered films one can clearly see that the rate drop with increasing inclination angle is faster in the later case: the HIPIMS rate at 3mTorr argon pressure and 90° angle is 32% of what was measured on the front face and the corresponding number for DC sputtering is only 24%. The relative difference is even larger for the 180° angle: 19% for HIPIMS vs 9% for DC. Increasing working gas pressure has a clear effect on the distribution of the sputtered material due to the scattering effects. Raising argon gas pressure from 3 mTorr to 10 mTorr decreases the mean free path for collisions of sputtered Cr atoms/ions with argon atoms from 5.2 cm down to 1.6 cm. This has an effect on thickness of produced coatings for both sputtering technologies (cf. Figure 4). However, even at 10 mTorr HIPIMS has a clear advantage over DC sputtering in terms of more uniform distribution of the sputtered material over the object being coated. The normalized deposition rate can be as much as 53% at 90° angle and 42% at 180° angle in the HIPIMS case. These results are in quantitative agreement with data reported for tantalum [17].

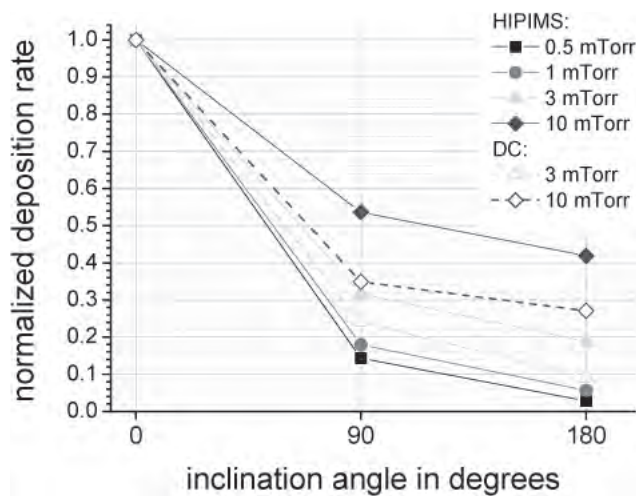


Figure 4: Deposition rates measured on substrates mounted at the inclination angle of 0° , 90° and 180° degrees. In each case data is normalized to the deposition rate on the sample facing the target (inclination angle equal to 0°).

The observed effect is ascribed to the presence of a significant amount of metal ions in the plasma that can be affected by the electric field configuration and, in this way, have a visible effect on the properties of the growing film (in this case - thickness). It has been shown for HIPIMS by Böhlmark et

al [8] that the highly ionized flux of the sputtered material can be effectively steered by magnetic fields. In the present case it is the substrate self-bias that affects some portion of the chromium ions from the plasma leading to increased coverage on samples tilted by 90° and 180° with respect to the target surface. The self-bias voltage (not shown) is typically in the range between 20V and 30V during the pulse on time, i.e., high enough to affect the movement of metal ions in the plasma. In the case of DC sputtering where the plasma contains a very low content of metal ions, the resulting coverage on the substrates inclined by 90° and 180° degrees is primarily due to scattering on the working gas atoms. This unique property of the HIPIMS plasma to some extent compensates for the drop in deposition rate: in the case of applications that deal with coating of 3D objects the actual deposition time should not scale up with the factor indicated by the rate drop measured on substrates facing the target.

Not only the normalized deposition rate is higher in the case of films deposited by HIPIMS at various inclination angles, but also the microstructure of the obtained films is drastically different from those prepared by DC sputtering. Figure 5 shows a set of SEM micrographs of the fracture cross-sections that reveal the microstructure of the films deposited at the inclination angle of 90° by HIPIMS (A, B and C) and DC (D, E and F). The average power increases from 1.5kW (A and D) to 5.5kW (C and F). Even though all the films are characterized by columnar structure, DC sputtered films appear extremely porous with columns growing at large tilt angle of about 40° degrees with respect to the surface normal, leading to a very open structure and high surface roughness. In contrast, films prepared by HIPIMS exhibit densely packed columnar structure with a typical column width of 80~100 nm and significantly lower tilt angle ($\sim 15^\circ$). Surface roughness is also lower than that of DC sputtered films. The lower tilt angle and denser microstructure typical for HIPIMS films are the result of enhanced ion impingement during film growth. Since the fraction of the chromium ions in the bulk of the plasma is significant in comparison with chromium atoms as indicated by the OES data discussed above, the electric field affects both the average angle at which sputtered atoms hit the substrate and the average ion energy.

As illustrated further in Figure 6, the microstructure of HIPIMS films is independent of the inclination angle, in contrast to the films deposited by DC sputtering. In this experiment the working gas pressure was raised to 10 mTorr in order to further reduce the column tilt and, in this way, facilitate comparison between the films grown by both the sputtering methods on inclined substrates. Even though the column tilt was reduced for the DC sputtered films, this classical deposition method is not capable of producing films of similar quality at all inclination angles studied. A series of micrographs shown to the right in Figure 6 (D, E and F) clearly indicates that the growth process is not the same for all three substrates. Only

on the substrate facing the target, a film of reasonable quality is obtained with DC sputtering, which is predominantly due to the fact that the intensity of the argon ion flux bombarding the substrate and the average energy of arriving Cr atoms is highest on this face (line-of-sight to the target). In contrast, the corresponding experiment performed with HIPIMS (Figures 6a, b and c) shows no major differences in the quality of all the three films on differently oriented substrates (apart from the thickness), indicative of significant and uniform ion bombardment that is, to the first order approximation, independent of the substrate orientation.

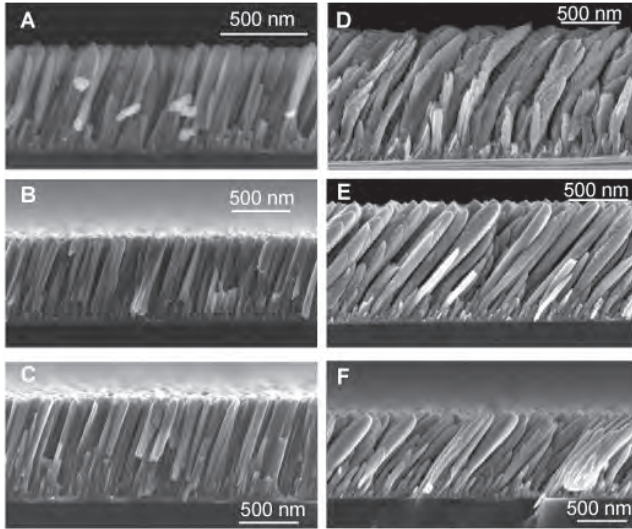


Figure 5: SEM micrographs of films deposited at inclination angle of 90 degrees: HIPIMS (left) vs DC (right). The average power levels and deposition times were as follows: (A) 1.5 kW/30 min., (B) 3.3 kW/30 min., (C) 5.5 kW/30 min., (D) 1.5 kW/30min., (E) 3.3 kW/15 min. and (F) 5.5 kW/10 min.

CONCLUSIONS

HIPIMS deposited chromium films on substrates at various inclination angles show more compact structure in comparison with DC sputtered films under the same conditions. Moreover, the loss of deposition rate from 0° to 90° and 180° inclination angle is significantly smaller in the case of HIPIMS. These results are of primary importance for applications that deal with coating of three dimensional objects. The obtained results indicate that deposition rate loss characteristic of HIPIMS technology is not necessarily as problematic as could be envisioned from the measurements performed on substrates facing the target.

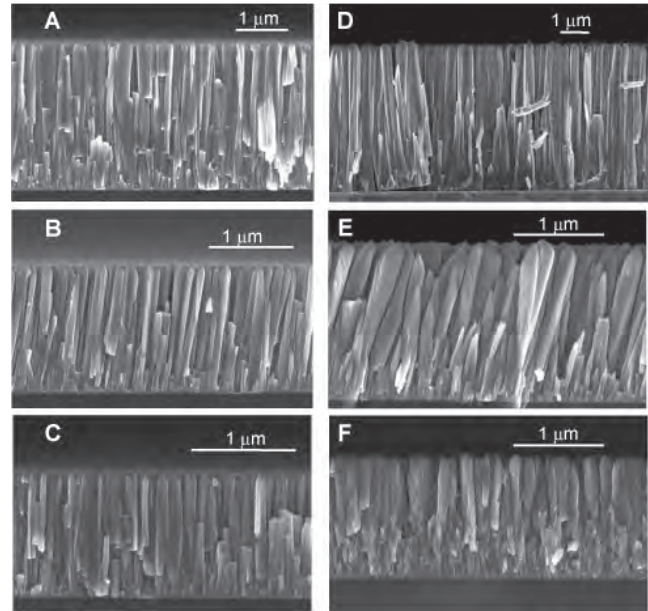


Figure 6: Film quality on various faces: HIPIMS (left) vs DC (right) at the same average power of 3.3 kW and argon gas pressure of 10 mTorr. (A) HIPIMS front (0°), (B) HIPIMS side (90°), (C) HIPIMS back (180°), (D) DC front (0°), (E) DC side (90°), (F) DC back (180°). Deposition time was 30 min. and 15 min. for HIPIMS and DC, respectively.

REFERENCES

1. U. Helmersson, M. Lattemann, J. Böhlmark, A.P. Ehasarian and J.T. Gudmundsson, "Ionized physical vapour deposition (IPVD): A review of technology and applications," *Thin Solid Films*, 513, 1, 2006
2. V. Kouznetsov, K. Macak, J.M. Schneider, U. Helmersson and I. Petrov, "A novel pulsed magnetron sputter technique utilizing very high target power densities," *Surface and Coatings Technology* 122, 290, 1999
3. J. Böhlmark, J.T. Gudmundsson, J. Alami, M. Latteman and U. Helmersson, "Spatial Electron Density Distribution in a High-Power Pulsed Magnetron Discharge," *IEEE Transactions on Plasma Science* 33 (2), 346, 2005
4. A.P. Ehasarian, R. New, W.-D. Münz, L. Hultman, U. Helmersson and V. Kouznetsov, "Influence of high power densities on the composition of pulsed magnetron plasmas," *Vacuum* 65, 147, 2002

-
5. J.T. Gudmundsson, J. Alami and U. Helmersson, "Spatial and temporal behaviour of the plasma parameters in a pulsed magnetron discharge," *Surface and Coatings Technology* 161, 249, 2002
 6. J. Böhlmark, J. Alami, C. Christou, A.P. Ehiasarian and U. Helmersson, "Ionization of sputtered metals in high power pulsed magnetron sputtering," *J. Vac. Sci. Technol. A* 23(1), 18, 2005
 7. B.M. DeKoven, P.R. Ward, R.E. Weiss, D.J. Christie, R.A. Scholl, W.D. Sproul, F. Tomasel and A. Anders, "Carbon thin film deposition using high power pulsed magnetron sputtering," *46th Annual Technical Conference Proceedings of the Society of Vacuum Coaters*, pp. 158-165, 2003
 8. J. Böhlmark, M. Östbye, M. Lattemann, H. Ljungcrantz, T. Rosell and U. Helmersson, "Guiding the deposition flux in an ionized magnetron discharge," *Thin Solid Films* 515, 1928, 2006
 9. I. Petrov, P.B. Barna, L. Hultman and J.E. Green, "Microstructural evolution during film growth," *J. Vac. Sci. Technol. A* 21(5), 117, 2003
 10. *Ionized Physical Vapor Deposition*, edited by J. A. Hopwood, Academic Press, San Diego, 2000
 11. J. Alami, K. Sarakinos, G. Mark and M. Wuttig, "On the deposition rate in high power pulsed magnetron sputtering discharge," *Applied Physics Letters* 89, 154104, 2006
 12. D. J. Christie "Target material pathways model for high power pulsed magnetron sputtering," *J. Vac. Sci. Technol. A* 23(2), 330, 2005
 13. J. Vlček, P. Kudláček, K. Burcalová and J. Musil, "High-power pulsed sputtering using a magnetron with enhanced plasma confinement," *J. Vac. Sci. Technol. A* 25(1), 42, 2007
 14. see: www.cemecon.de
 15. A.P. Ehiasarian, R. New, P. Eh. Hovsepian, J. Böhlmark, J. Alami and U. Helmersson "Influence of pressure and power on the composition and time evolution of plasmas in high power impulse magnetron sputtering," *47th Annual Technical Conference Proceedings of the Society of Vacuum Coaters*, pp. 437-442, 2004
 16. J. Böhlmark, U. Helmersson, M. VanZeeland, I. Axnäs, J. Alami and N. Brenning, "Measurement of the magnetic field change in a pulsed high current magnetron discharge," *Plasma Sources Science and Technology* 13, 654, 2004
 17. J. Alami, P. Eklund, J.M. Andersson, M. Latteman, E. Wallin, J. Böhlmark, P. Persson and U. Helmersson, "Phase tailoring of Ta thin films by highly ionized pulsed magnetron sputtering," *Thin Solid Films* 515, 3434, 2007